

Reprinted from

# EARTH AND PLANETARY SCIENCE LETTERS

---

Earth and Planetary Science Letters 133 (1995) 475-491

The upper Olduvai geomagnetic field reversal from Death Valley,  
California: a fold test of transitional directions

John W. Holt \* , Joseph L. Kirschvink

Division of Geological and Planetary Sciences, California Institute of Technology, Pasadena, CA 91125, USA

Received 8 August 1994; accepted 22 May 1995





ELSEVIER

Earth and Planetary Science Letters 133 (1995) 475-491

---

---

EPSL

---

---

# The upper Olduvai geomagnetic field reversal from Death Valley, California: a fold test of transitional directions

John W. Holt \* , Joseph L. Kirschvink

Division of Geological and Planetary Sciences, California Institute of Technology, Pasadena, CA 91125, LISA

Received 8 August 1994; accepted 22 May 1995

## Abstract

High-resolution records of the upper Olduvai geomagnetic field reversal were obtained from two localities within steeply dipping lacustrine sediments of the Confidence Hills, southern Death Valley, California. The difference in bedding attitude between the two localities allowed us to perform a fold test of both transitional and non-transitional paleomagnetic directions. This is the first positive fold test obtained for transitional directions from any geomagnetic field reversal. In addition, variations in lithology allowed a comparison of transitional records from different sedimentary environments. Alternating-field and thermal demagnetization reveals that most samples have either single or simple two-component magnetizations. The low-coercivity, low-blocking temperature component is most likely held by large multidomain grains of magnetite, and aligns with the present-day field when uncorrected for bedding orientation. The high-coercivity component is held primarily by single- and pseudo-single-domain titanomagnetite, as determined from standard magnetic studies and electron microscopy. This component is interpreted as a primary magnetic signature based on the presence of stratigraphically bound reversals in the tilt-corrected data and positive reversal tests. Short-term field variations can be correlated between the two records, and differences are readily explained by the recording process inherent to the two sedimentary environments. The sampling site is located within one of the "preferred" bands of transitional virtual geomagnetic poles (VGP's) [1-3], yet the transitional VGP paths from both localities are clustered within two primary longitudinal bands which are approximately 90° away from the sampling site longitude: one lies over the Atlantic ocean (10°-50°W), and the other, antipodal to this (130°-170°E). These bands are also inconsistent with eight previous studies of the upper Olduvai transition [4-9,3,10]. When all reported studies of this reversal are examined, however, no global consistency exists. Instead, the transitional VGP's are better grouped in a sampling site reference frame.

## 1. Introduction

One of the most exciting and controversial developments in recent geomagnetic research has been the observation that virtual geomagnetic poles (VGP's) during polarity transitions appear confined to longitudinal bands centered over the Americas and Australasia [1-3]. This has stirred much debate regard-

ing both the statistical significance of this observation [2,11-15] and the physical mechanism responsible for it. Laj et al. [2] claim that there may be a link between these paths and structure near the core-mantle boundary. They point out seismic evidence for colder regions in the lower mantle, and models of fluid flow in the outer core which show the region underlying these proposed paths to be ones where N-S flow predominates. Such correlations have profound implications. If these links turn out to be real,

\* Corresponding author

then geomagnetic phenomena in the core may eventually be tied to mantle dynamics [16]. However, there are at least two important issues relevant to this debate which need to be resolved. First, Egbert noted that preferred paths could be the result of nonuniform sampling site distribution [17]. Indeed, many of the sites with detailed records of Pliocene and Pleistocene reversals tend to be located in Europe and the West Pacific, roughly  $90^\circ$  away from the proposed longitudinal bands. Second, and more fundamental, is whether or not the studies which are used for these compilations have provided accurate records of transitional field behavior. Few of the transition studies published so far have provided any of the classical paleomagnetic tests which can place constraints on when the magnetizations were acquired.

A recent investigation into the relationship between the anisotropy of anhysteretic remanence (AAR) and paleomagnetic remanence implied that these sediments may not accurately record magnetic field directions during periods of low field intensity [18]. While the classical paleomagnetic tests performed in the study presented here do not directly address anisotropy issues, they place important constraints on such data and may be crucial to their interpretation. In this paper, we present multiple records of the upper Olduvai reversal obtained from these sediments which agree across a distance of 1.6 km, despite folding and changes in sedimentary environments.

## 2. Geologic setting

### 2.1. Tectonic setting

The Confidence Hills are located in southern Death Valley, California along the eastern flank of the Owlshhead Mountains (Fig. 1). Death Valley is in the southwestern part of the Basin and Range geological province of North America, an area of late Cenozoic extension. The deep central segment of Death Valley is interpreted to be a pull-apart structure developed as a result of tension between segments of the right-lateral Death Valley and Furnace Creek fault zones [19].

An asymmetrical anticlinorium forms the bulk of the Confidence Hills, the axis of which runs nearly parallel to the western strand of the southern Death Valley fault zone. The Pliocene to early Pleistocene sedimentary rocks exposed there have been folded and uplifted as much as 200 m above the valley floor [20,21]. Bedding is well preserved with dips ranging from approximately  $20^\circ$  to slightly overturned.

### 2.2. Rocks of the Confidence Hills

The sedimentary rocks sampled for this study belong to a fine-grained part of the Funeral Formation in southern Death Valley, California [22,20], and are within the proposed Confidence Hills Formation [23]. These rocks are dominated by fine-grained

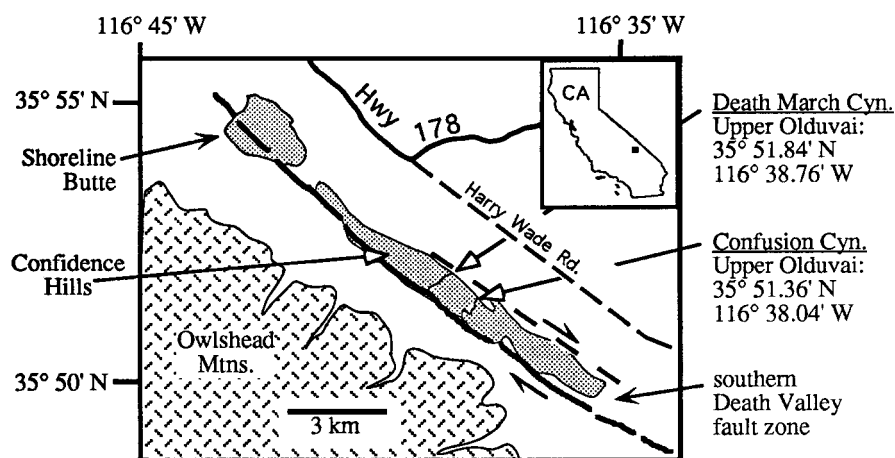


Fig. 1. Location map of sampling sites within the Confidence Hills in southern Death Valley. Partially adapted from geologic map of Wright and Troxel [20].

siliciclastic sediment and bedded gypsum/anhydrite deposited in marginal subenvironments of a saline lake [23]. There are no fossils present in these sediments, and no indicators of bioturbation or chemical alteration. Active erosional channels which cut nearly perpendicular to the bedding strike provide fresh outcrop in which to examine the stratigraphic sequence and collect relatively unweathered samples. We concentrated our efforts on two major erosional channels 1.6 km apart, informally named Death March Canyon and Confusion Canyon (Fig. 1).

Each section is bounded by the western strand of the southern Death Valley fault at its base, and an angular unconformity at the top. The measured sections begin above the most severe disruption near the fault zone. The only stratum that can be visually correlated between the two sections is a 40-cm-thick grey ash layer, located at 90 m in Confusion Canyon and at 144 m in Death March Canyon. This ash layer has been chemically fingerprinted as the Huckleberry Ridge ash [24], and provides a key time constraint for the determination of specific polarity reversals in these sections. The Huckleberry Ridge tuff has been dated at  $2.057 \pm 0.008$  Ma using the single-crystal  $^{40}\text{Ar}/^{39}\text{Ar}$  method [25].

### 2.3. Sedimentology of the upper Olduvai interval in Confusion Canyon

In Confusion Canyon, the upper Olduvai transition is recorded in fine-to medium-grained, well-sorted sandstone with some thin, clay-rich layers. Bedding geometry is sheet-like, without cross-lamination. Bedding thicknesses range from a few centimeters to approximately 10 cm, with the majority being 5-10 cm. Thin-section examination reveals that the rocks are primarily composed of angular to sub-angular grains of quartz, feldspar, and opaque minerals with no signs of weathering. These grains were probably eroded from the nearby Mesozoic granitic rocks of the Owlshhead Mountains (Fig. 1). Using X-ray diffraction, Beratan et al. [23] found that the dominant clay-size minerals are plagioclase feldspar (approximately An-67), quartz, and mica, with minor amounts of smectite. This is consistent with deposition in an arid environment, where physical weathering is greatly dominant over chemical weathering. The sediments in this interval are inter-

preted to have been deposited on a sandflat, marginal to a saline lake, supplied by a fringing alluvial fan [23]. This is a depositional environment in which floodwaters disperse as unchanneled sheetfloods across a flat sand plain. Individual beds are probably deposited in single events. The presence of mudcracks indicate that in some instances subaerial exposure occurred between events. Bedding attitude in the transition zone is  $S74^\circ E/82^\circ SW$  (overturned).

### 2.4. Sedimentology of the upper Olduvai interval in Death March Canyon

In Death March Canyon, the upper Olduvai transition is recorded in banded anhydrite, which is composed of very-thin-to thin-bedded (from a few millimeters to several centimeters) anhydrite interbedded with siltstone and some fine-grained sandstone. Bedding geometry is sheet-like, without crosslamination. Bedding thickness ranges from a few millimeters to approximately 10 cm, with the majority being less than 5 cm. The siliciclastic layers contain essentially the same mineralogy as the rocks in Confusion Canyon, with smaller grain sizes. These sediments are interpreted to have been deposited in a saline mudflat marginal to a saline lake [23]. This indicates a more continuous depositional regime than the upper Olduvai interval in Confusion Canyon. Bedding attitude in the transition zone is  $N64^\circ W/45^\circ NE$ .

### 2.5. Deposition rates

An average sedimentation rate was determined for the Olduvai subchron (1.95-1.79 Ma, [26]) in each canyon from magnetostratigraphy alone, and this is 28.4 cm/kyr in Confusion Canyon, and 33.1 cm/kyr in Death March Canyon, without any evidence for significant hiatuses. As will be shown later in detail, we were able to match short-term field variations in the two records and estimate the relative deposition rates between the two canyons for the interval spanning the upper Olduvai reversal. This method shows that during this interval, the average deposition rate in Death March Canyon was approximately 54% higher than that in Confusion Canyon, consistent with the sedimentary environment interpretations of Beratan et al. [23].

3. Methods

3.1 Sampling

Samples were collected with a gasoline-powered drill using air-cooled, diamond-tipped, 25 mm diam-

eter coring bits. Sample orientation was determined using a brass orienting sleeve and a magnetic compass. A sun compass was determined to be unnecessary. Broken samples were repaired in the laboratory using alumina cement, and most samples were trimmed to a maximum length of 22 mm.

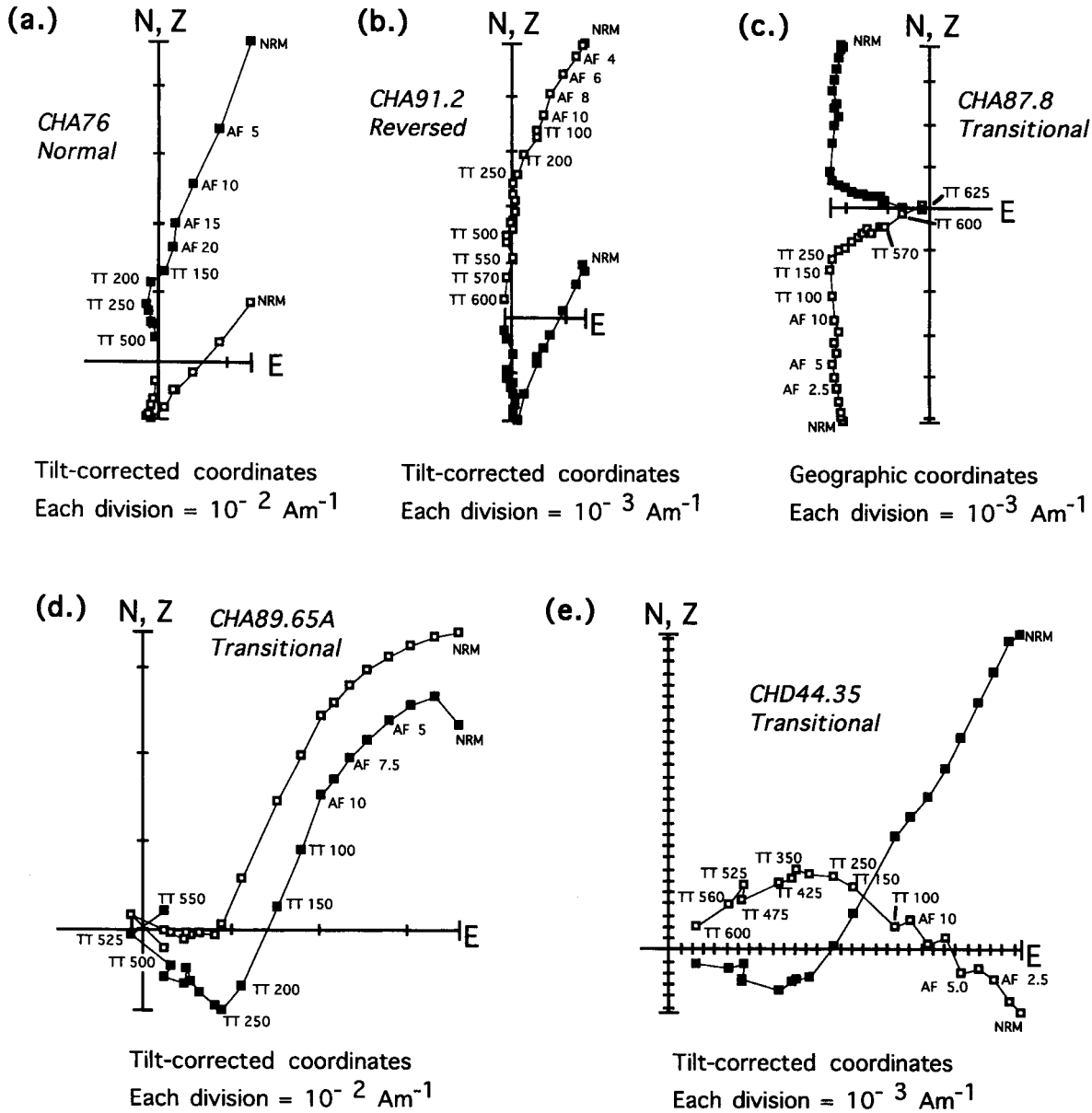


Fig. 2. Sample demagnetization. Orthogonal projections of declination onto the horizontal plane (solid squares) and inclination onto the vertical plane (open squares) for typical two-component samples of (a) normal, (b) reversed, and (c-e) intermediate polarities.

### 3.2. Measurements

#### Paleomagnetic directions

Measurements were made using a computer controlled, magnetically shielded SQUID magnetometer with a background noise level of  $5 \times 10^{-12}$  Am<sup>2</sup> located within a magnetically shielded room. All samples were subjected to both static three-axis alternating field (AF) and thermal demagnetization. AF demagnetization was performed first on all samples, usually up to a maximum of 10 mT in 1.25 mT steps. Thermal demagnetization was then used, from 100°C to 400°C in 50° steps, and then from 425°C to a maximum of 625°C in 25° steps. Multiple magnetization components were isolated using least-squares principal component analysis [27]. Due to the steep dip of bedding in these sections, a present-day overprint is easily distinguished from both normal and reversed primary magnetic directions.

#### Rock magnetic measurements

Rock magnetic studies were undertaken in order to constrain the mineralogy and morphology of the magnetic components of these rocks. Small portions (approximately 0.05 g) of samples throughout the transition zones were disaggregated, placed in a 1 ml plastic epindorph tube and sealed. Experiments included (1) an acquisition of anhysteritic remanent magnetism (ARM) in a 100 mT alternating field, with progressively stronger background biasing fields between 0 and 2 mT as done by Cisowski [28], (2) the progressive AF demagnetization of the ARM after the 2 mT ARM acquisition, (3) the progressive AF demagnetization of a 100 mT isothermal remanent magnetization (IRM), and (4) IRM acquisitions in pulsed fields up to 800 mT.

Magnetic material was extracted from two samples within each of the transition zones and two outside of each transition zone for direct analysis. Extraction was accomplished by gentle disaggregation, dissolution in weak acetic acid, and magnetic separation. Analysis techniques included imaging by scanning electron microscope (SEM) with energy dispersive spectral (EDS) analyses and by transmission electron microscope (TEM) with spot diffraction analyses.

Magnetic susceptibility of all samples was measured using a Bartington M.S.2 susceptibility meter before, during, and after heating.

#### Paleointensity measurements

Anhysteritic remanent magnetization (ARM) was induced in samples across the upper Olduvai transition after demagnetization in order to normalize the intensity of the primary magnetic component. The samples were subjected to a 50  $\mu$ T biasing field with an alternating field of 80 mT peak. Relative paleointensity was estimated by normalizing the primary magnetization component by the induced ARM. This was preferred over susceptibility normalization because the carrier of the ARM is more likely to be the same as the carrier of the primary remanence direction [29].

## 4. Results

### 4.1. Demagnetization

The intensity of the NRM for these samples was on the order of  $10^{-1}$  A/m. Progressive demagnetization, as described above, allowed us to resolve multi-

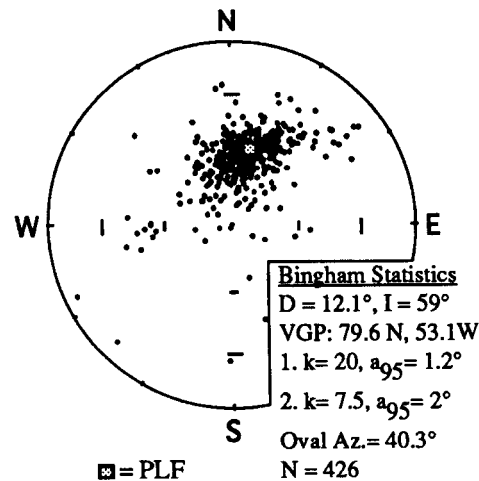


Fig. 3. Overprint directions. Equal area projections of overprints from all samples which exhibited two-component magnetizations. Closed circles and PLF (present local field) represent lower hemisphere projections. Bingham statistics show that the overprint is distributed near the present-day field direction for this location. ( $D$  = declination east of north;  $I$  = inclination, positive downward;  $k$  = precision parameter;  $N$  = number of samples.) As discussed in the text, this overprint is removed after AF demagnetization to 10 mT and thermal demagnetization to 250°C, and is therefore interpreted as a viscous remanent magnetization (VRM) held by multidomain magnetite and/or maghemite.

ple components of magnetization. For the vast majority of the samples, there were two clear components -- a primary magnetization and a present-day field overprint (Fig. 2). A few samples (some reversed-polarity samples in the upper part of the Death March Canyon section) exhibited single-component primary magnetizations (Fig. 2c), without any apparent overprint. The magnetization of some samples became essentially zero or random at approximately 525°-550°C, and heating was discontinued when this condition was reached.

The overprint, which is a low coercivity, low blocking temperature component, is removed by AF demagnetization at 10 mT and thermal demagnetization at 250°C. An equal area plot showing the direction of the low-coercivity component from all samples (normal, reverse, and transitional) showing two components is shown in Fig. 3. The mean direction calculated from Bingham statistics [30] is very close

to the present-day field for this locality, so this component is interpreted as being a viscous remanent magnetization (VRM). The demagnetization characteristics of this component indicate that it is held primarily by multi-domain magnetite grains and partially by goethite and/or maghemite.

In Fig. 4, a typical sample's magnetization versus demag step is plotted. It is apparent that there is little overlap between the coercivity spectra of the two components of magnetization. The plot shows that the overprint component is not affecting the primary magnetization after the 250°C thermal step, and there is no consistent component in the direction orthogonal to the primary and overprint directions.

#### 4.2. Rock magnetism

Fig. 5 shows a coercivity spectrum with results of the ARM Lowrie-Fuller test [31] measured from a typical

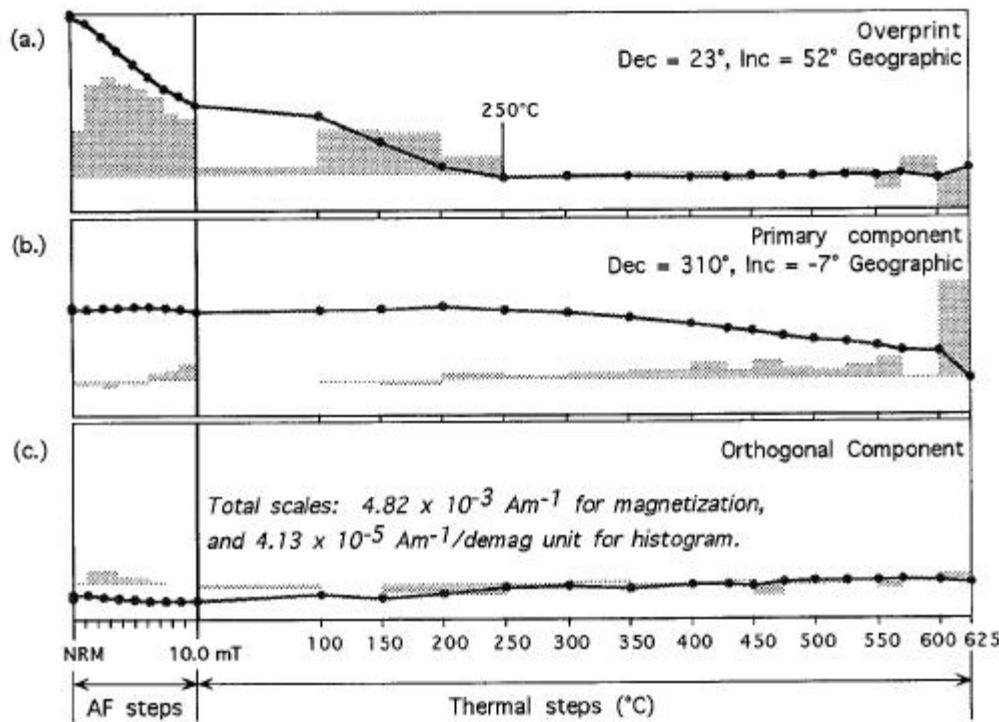


Fig. 4. Sample magnetization versus demag step. The ratio of  $J/J_0$  is plotted separately for each component, as a function of demagnetization step: (a) the overprint, (b) the primary direction, and (c) a calculated component in the direction orthogonal to these two components. Erratic behavior in the orthogonal component indicates a lack of overlap between the overprint and primary directions. The removal of the overprint direction by the 250°C thermal step is apparent, as is the small amount of overlap between the coercivities of the two components. The shaded boxes represent the derivative of the  $J/J_0$  line, indicating the coercivity/blocking temperature spectrum for that component.

sample. For the IRM acquisition data, roughly 95% of the intensity is acquired after exposure to peak fields of less than 300 mT. This is indicative of magnetite with a small portion of higher coercivity material, such as hematite. The positive Lowrie-Fuller test (demag of ARM > demag of IRM) indicates that the primary magnetic carrier is relatively fine-grained material (single- or pseudo-single-domain size).

The results of direct SEM and TEM analyses indicate that titanomagnetite constitutes the magnetic fraction responsible for holding the stable primary remanence. One fraction consists of single- to pseudo-single-domain sized grains [32], ranging from 50 nm to 3  $\mu\text{m}$  in size. These are either equant or slightly elongate prismatic grains, or clearly equant octahedral titanomagnetite crystals (with Ti/Fe ratio of approximately 0.25, from EDS analysis). Another fraction consists of tabular magnetite and titanomagnetite grains which are approximately 30-100  $\mu\text{m}$  across. This larger size fraction is clearly multi-domain [32], and is probably the primary carrier of the magnetically soft overprint. In support of this conclusion, none of these large magnetic grains were found in extracts from reversely magnetized samples above the Olduvai subchron in Death March Canyon which exhibited no overprint.

There was no detectable correlation of magnetic susceptibility with stratigraphic position. Susceptibility changes due to heating were less than 10%, without any consistent pattern. This indicates that there were no significant changes in mineralogy during heating. In samples which exhibited erratic behavior above approximately 525-550°C, some minor new magnetic phases may have formed during heating at higher levels but the primary remanence directions were well established by this level.

#### 4.3. Magnetostratigraphy

Plots showing the overall magnetostratigraphy from both canyons are shown in Fig. 6 correlated with the Geomagnetic Polarity Time Scale (GPTS) adapted from Harland et al. [33] with the astronomically calibrated ages of Hilgen [26]. The Reunion event is found in the lower part of each section, and the entire Olduvai subchron is recorded above the Huckleberry Ridge ash.

#### 4.4. Non-transitional directions (fold and reversal tests)

Two critical tests of the primary directions were performed on these sedimentary rocks -- a reversal test and a fold test. Fig. 7 shows non-transitional data from each section plotted on equal-area diagrams. Non-transitional data were restricted to time-equivalent strata from each section (163-260 m in Death March Canyon, and 102-195 m in Confusion Canyon, excluding the transitional intervals defined below). The reversal test compares the mean directions of the normally and reversely magnetized strata, in order to test for antiparallel field orientations. The formulation of McFadden and McElhinny [34] was used to characterize this test. Both sections pass the common distribution test; therefore, the null hypothesis that the directions are antiparallel cannot be rejected at the 90% confidence level. For the analytical test, with one mean reversed through the origin, Death March Canyon's means have an observed angular difference of 2.98° and a calculated critical angle (95% confidence) of 7.51°. For Confusion Canyon, the observed angular difference is 1.43° with a critical angle of 5.85°. Thus, both sections also pass the analytical test, with a "B" quality classification [34].

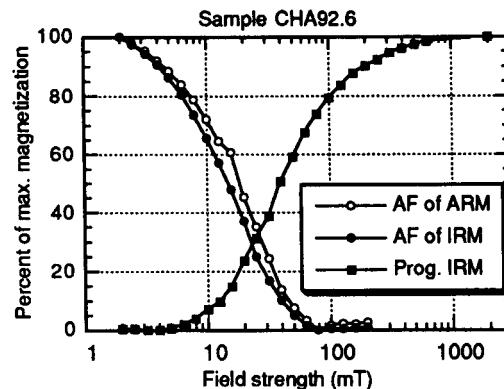


Fig. 5. IRM/ARM acquisition and demagnetization. A typical coercivity distribution for a sample from Confusion Canyon. Samples from throughout the section exhibit similar patterns, as do all tested samples from Death March Canyon. Data for the IRM acquisition and AF demagnetization of the IRM are shown with open circles. The open circles show the AF demagnetization of the of the ARM acquired in a 2 mT direct current biasing field with a 100 mT (max) alternating field.



The fold test compares primary directions from each section before and after tilt-correction to determine if the remanence was acquired before structural folding of the strata. This was implemented by comparing the same non-transitional directions as used in the reversal test (Fig. 7). Before tilt-correction, the means from each canyon are distinctly different.

After tilt-correction, the means are statistically indistinguishable, according to the method of Fisher [35]. This verifies that the sediments in both sections acquired their remanence before tilting of the strata.

The positive results from these two stability tests, along with the fact that stratigraphically bound polarity reversals are contained within the sections, show

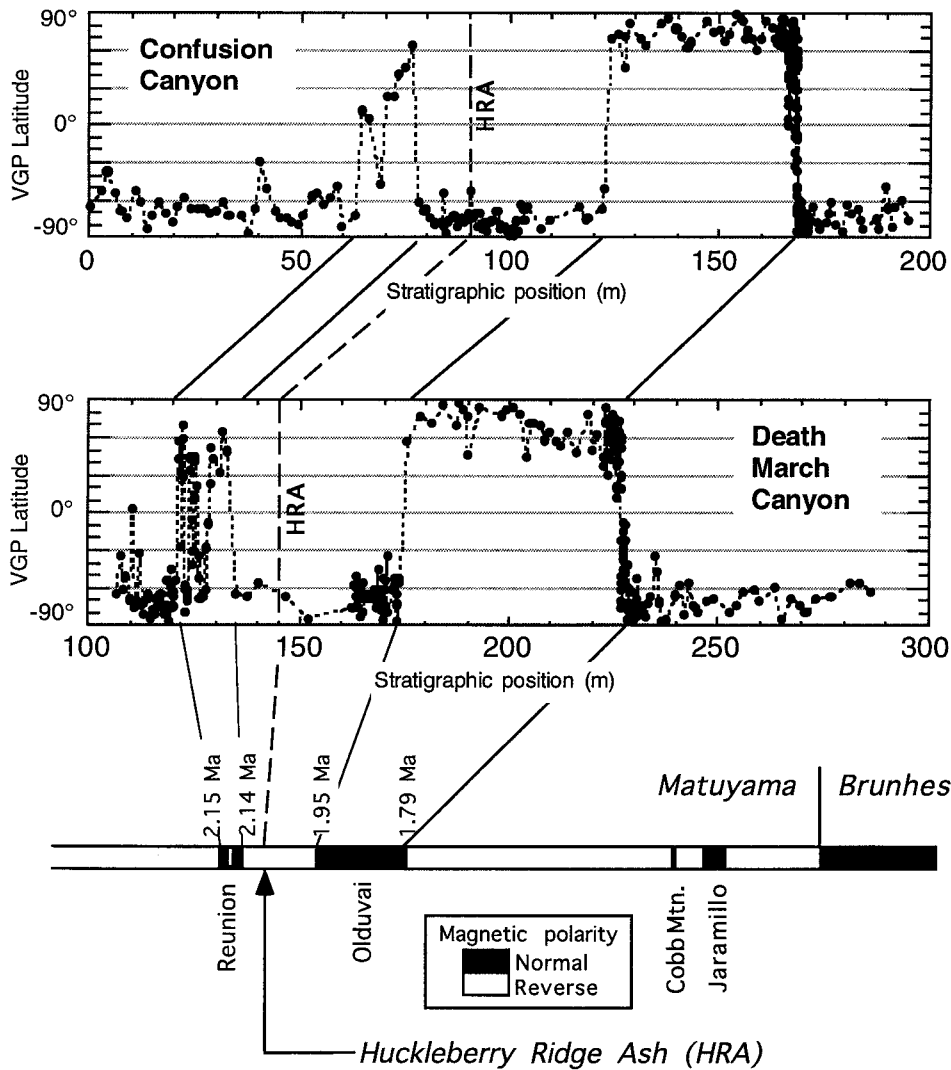


Fig. 6. Magnetostratigraphy. VGP latitude as a function of stratigraphic position for both sections, compared with the Geomagnetic Polarity Timescale (GPTS), adapted from Harland et al. [33], with ages from Hilgen [26]. The location of the Huckleberry Ridge ash (- 2.057 Ma, [25]) is shown for reference.

that these directions were acquired by the sediments at or soon after deposition. Since there are no significant changes in lithology or structure across the

transition zone in either canyon, it follows that the sediments deposited during the transition should also pass the fold test, assuming that they had the ability

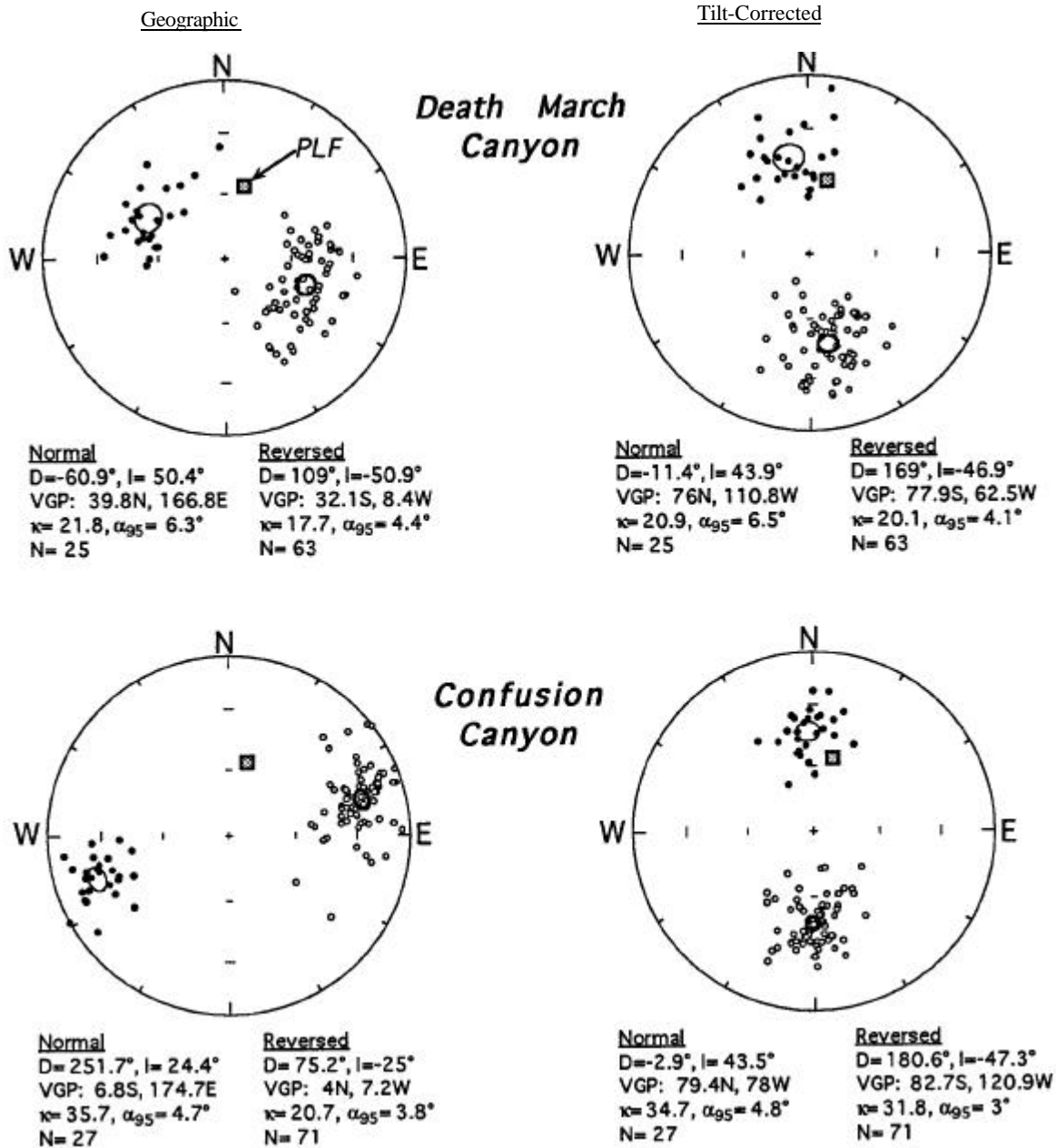


Fig. 7. Non-transitional data, reversal tests, and fold test. Equal area plots of the non-transitional directions from both canyons—closed circles represent lower hemisphere projections, open circles represent upper hemisphere projections. Both sections pass the reversal tests of McFadden and McElhinny [34], and the fold test as discussed in the text. (D = declination east of north; I = inclination, positive downward;  $k$  = precision parameter; N = number of samples.)

to record ambient magnetic field directions during the period of reduced field intensity. The actual changes in field direction are used to qualitatively assess the agreement of the two records within the transition zone, as discussed below.

The expected geocentric axial dipole inclination for the latitude of the Confidence Hills is  $55.3^\circ$ . The mean non-transitional inclination from both sections is approximately  $44^\circ \pm 6^\circ$  for normally magnetized

strata and  $-47^\circ \pm 4^\circ$  for reversely magnetized strata (Fig. 7). Due to the uncertainties in the expected inclination due to the non-dipole inclination anomaly [36] and the error bars on the mean inclination, we can only estimate inclination shallowing due to compaction to be in the range  $0-15^\circ$ . Therefore, the exact effect on transitional directions due to any inclination shallowing is unknown. On the other hand, even if the maximum amount is chosen there is

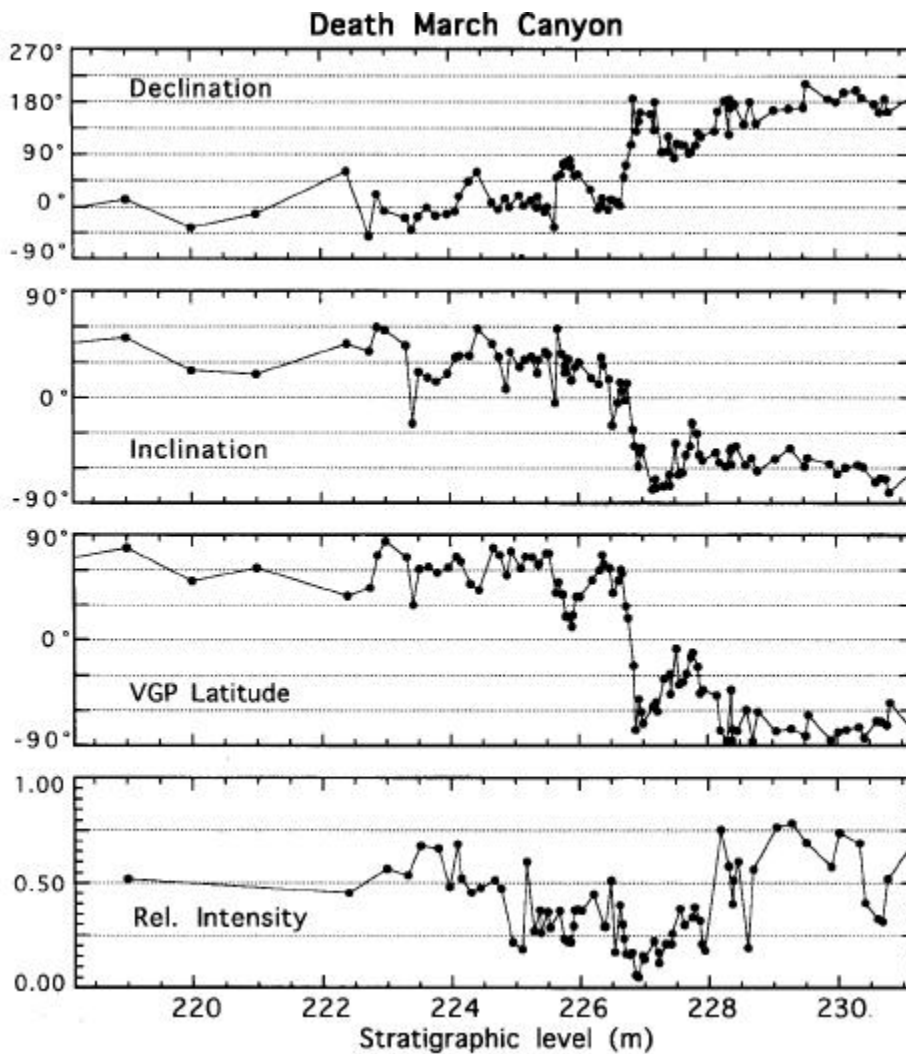


Fig. 8. Transitional data. Declination, inclination, VGP latitude, and relative intensity (TT250/ARM) plotted as a function of stratigraphic position across the upper Olduvai transition, for (a) Confusion Canyon, and (b) Death March Canyon. The intervals used in each canyon were selected in order to match the obvious central feature, which is most clearly seen in the declination record and appears to be an aborted reversal. The Death March Canyon stratigraphic interval is 54% longer for the overall transition, implying that the average sedimentation rate there during this interval was 54% higher than in Confusion

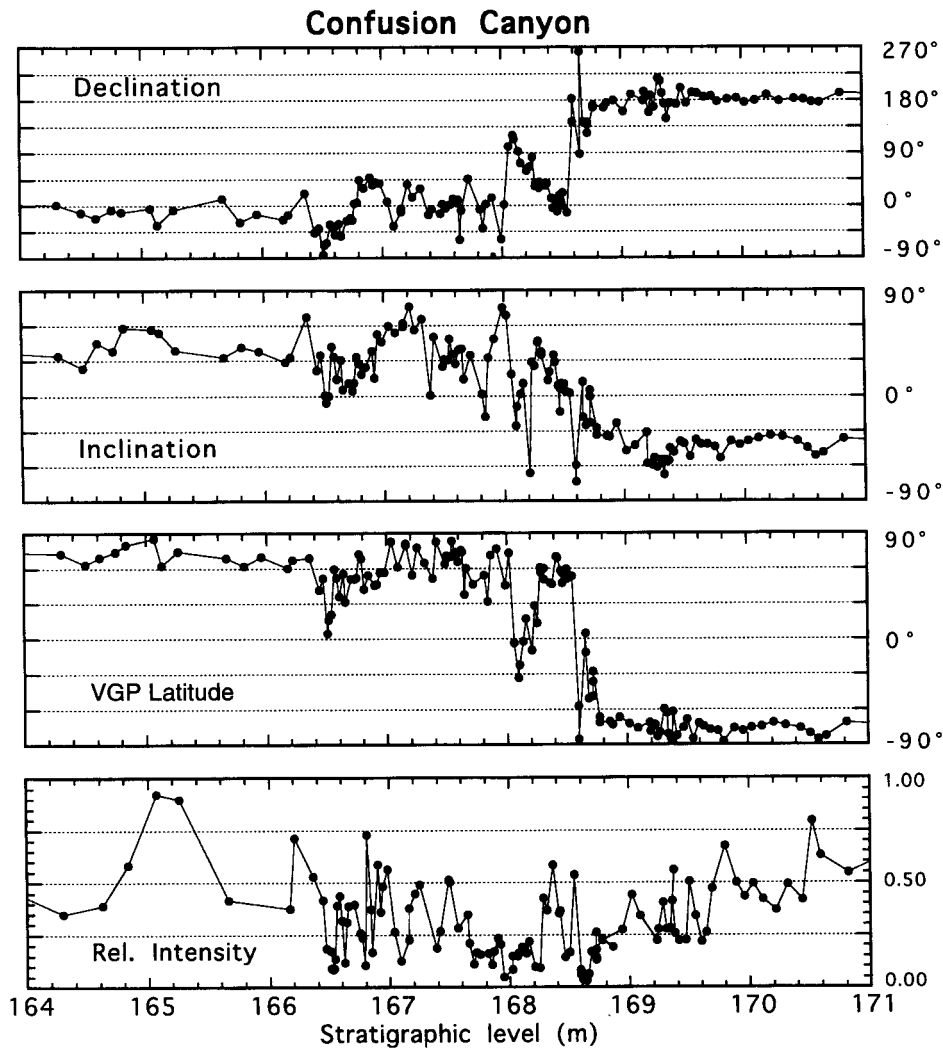


Fig. 8 (continued).

not a significant change in the major results of this study.

#### 4.5. Transitional data

Detailed plots of declination, inclination, virtual geomagnetic pole (VGP) latitude, and relative paleointensity through the upper Olduvai transition zone are plotted in Fig. 8 as a function of stratigraphic level.

These intervals were defined by the broad de-

crease in paleointensity surrounding the main part of the reversal, and also by large fluctuations in the VGP latitude. Short-term variations in the field directions were used to adjust the chosen stratigraphic intervals from each canyon in order to obtain the best match. This resulted in a 13 m section of Death March Canyon being correlated with a 7 m section of Confusion Canyon. If this match is correct, then Death March Canyon had a 54% higher sedimentation rate than Confusion Canyon during this interval. Based on these constraints and a slightly tighter

transitional zone than shown in Fig. 8, estimates of the duration of the upper Olduvai reversal range from approximately 9-18 kyr.

The primary feature, an aborted reversal, is very distinctive, so we are confident that we are not correlating random directions. This aborted reversal includes a fast jump to low VGP latitudes followed by a gradual decay of the field back to normal polarity, and then a sudden jump to reversed polarity, followed by a brief rebound. This is very similar to the general VGP latitude behavior during the

upper Olduvai reversal reported by Tric et al. [3] and Lee [10]. The sudden nature of the onset and termination of this feature could be due to rapid field behavior or to depositional hiatuses. There is no field evidence for any hiatus more significant than a typical bedding plane, however, so we feel that the field must be changing at least somewhat rapidly.

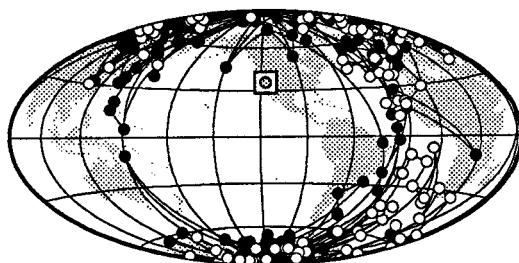
On the other hand, there are differences in the way the two sections record the transitional data. The sandflat depositional environment of Confusion Canyon produces a record that shows small jumps in



(a) Confusion Canyon



(b) Death March Canyon



(c) Combined VGP's

Fig. 9. VGP paths. VGP's are calculated for the transition zone data shown in Fig. 8, and are shown here on Hammer-Aitoff projections of the earth, centered on the sampling site meridian ( $116.5^{\circ}\text{W}$ ). Latitude and longitude grid spacings are  $30^{\circ}$ . Results for the individual localities are shown for (a) Confusion Canyon, and (b) Death March Canyon. (c) The combined paths illustrate the agreement of the transitional directions between the two locations. The sampling site location is indicated with a boxed data symbol.

the field directions, most of which are correlatable to directions in the more continuous deposition of the saturated mudflat environment of Death March

Canyon. The individual beds in Confusion Canyon seem to record the field direction at the time of the deposition of the bed, with "lock-in" occurring

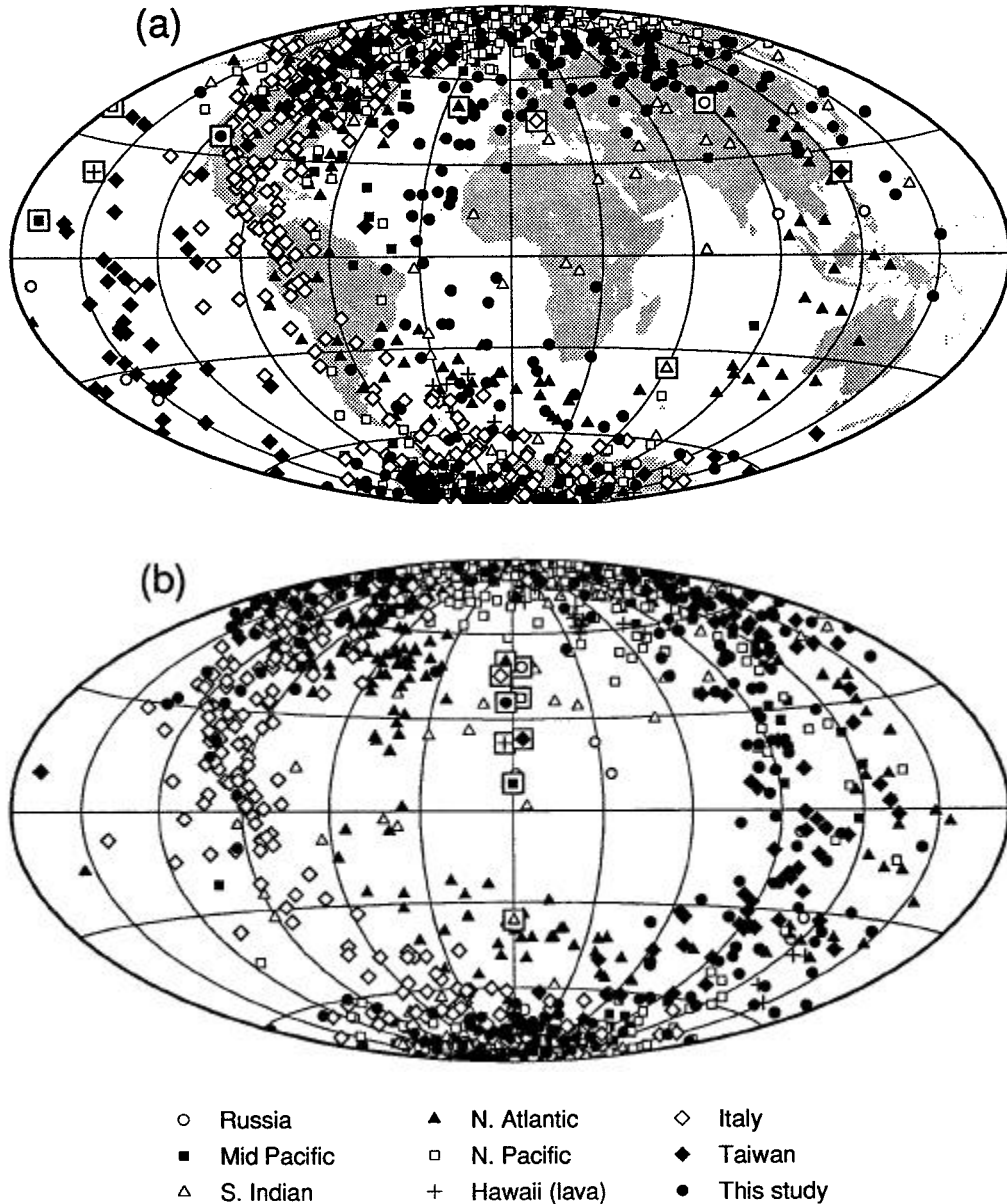


Fig. 10. All upper Olduvai data. Previous data is from Russia [4], the middle Pacific Ocean [5], the Southern Indian Ocean [6], the North Atlantic [7], the North Pacific [8], Hawaii (lava) [9], Italy [3], and Taiwan [10]. VGP's from all studies in addition to those from this study are plotted together. Sampling sites are indicated by boxed data symbols for each respective study (staggered for display in order to minimize overlap). (a) Hammer-Aitoff projection centered on 0° longitude. Latitude and longitude grid spacings are 30°. (b) The same data plotted with sampling sites shifted to a common longitude, which is the center of the projection.

before deposition of the next bed. Similarly, the return of VGP latitudes to low negative values (rebound) after the main reversal, which occurs from 227 to 227.8 m in Death March Canyon, appears to be only partially recorded in Confusion Canyon from 168.6 to 168.8 m.

The intensity of magnetization at the 250°C thermal step (the point at which the overprint was entirely removed in most samples) is shown normalized with these ARM values across the transition in Fig. 8. The period of reduced field intensity is longer than the time during which the field reverses polarity. This is in agreement with other studies of the upper Olduvai [8,3]. The most noticeable feature of intensity during the middle of the reversal is the brief rise which accompanies the gradual return of VGPs to high latitudes after the aborted reversal (168.2 - 168.6 m in Confusion Canyon; 226-226.5 m in Death March Canyon)

#### 4.6. VGP paths

The tilt-corrected transitional VGPs from each section are displayed on global projections in Fig. 9. The aborted reversal produced VGPs along the path which is to the west of the sampling site, while the full reversal occurred along the path to the east of the sampling site. The rebound after the main reversal, which was recorded with more detail in Death March Canyon, also transgressed along the path east of the sampling site. The similarity of the two records is quite evident when the tilt-corrected data from both sections are combined in one VGP plot (Fig. 9c).

## 5. Discussion

### 5.1. Comparison with other studies

An interesting result is that this sampling location lies within one of the longitudinal bands "preferred" by VGPs during reversals [1-3], whereas transitional VGPs trace out paths which are approximately 90° away from the sampling site longitude in either direction. We have plotted data from all available published records [37] of the upper Olduvai in Fig. 10a. VGP longitudes of Lee [10] were corrected

from original data. There is no clear geographic consistency in transitional paths produced for this reversal; furthermore, they do not particularly lie along the longitudinal band of the Americas or the antipodal band. Also apparent in Fig. 10a is the observation that VGP longitudes resulting from our study are distinctly different from those of other detailed studies of the upper Olduvai.

A noteworthy similarity exists between the shifts in VGP latitudes found in our study and those reported by Tric et al. [3]. In both cases, there is a pronounced drop in VGP latitudes followed by a gradual recovery which is then followed by a sudden change in polarity with a brief rebound.

The transitional data from most of these studies appear to be better correlated in sampling site coordinates than in geographical coordinates. The transitional data is plotted with a common sampling site longitude in Fig. 10b and comparison with Fig. 10a shows that the data is slightly better grouped in this reference frame. The VGP paths tend to be located approximately 90°-120° away from the sampling site longitude for this reversal, with the notable exception of the study by Clement and Kent [7]. It should be noted that all of these records were obtained from sediments except for the study by Hoffman [9], which used volcanic rocks.

### 5.2. Reliability of transitional directions

Mechanisms for producing this phenomenon in sediments have been proposed, and involve the reduction in field intensity which accompanies reversals. The ability of the earth's field to align elongate magnetic particles in sediments, whether before, during, or after deposition, may become insufficient to overcome the gravitational force on the particle, resulting in shallow inclinations [38,15]. A mixture of elongate and equant particles could produce the same result through a slightly different mechanism -remanence may be dominated by field-oriented equant grains during normal intensity, and by gravity-oriented elongate particles during periods of low field intensity [18].

Determining whether either of these processes are actually occurring is a difficult problem, however. A preliminary anisotropy study was performed with the goal of addressing this issue [18]. The results indi-

cated that remanence declinations for low-latitude VGP's may follow the directions of the maximum horizontal axes of the ellipsoids of anisotropy of anhysteretic remanence (AAR) more closely than those of high-latitude VGP's. This was interpreted to mean that during the transition when the field intensity is low, remanence is dominated by elongated grains aligned by forces other than the geomagnetic field, since equant grains would be more randomly oriented. While this is a plausible mechanism for producing VGP's which are far from the sampling site meridian, it has difficulty explaining the consistent behavior of the two records. The progressive and distinctive changes in direction during the reversal are similar in both sections, recording the aborted reversal, the main polarity shift, and the brief rebound. It is possible that the inclinations were severely shallowed while the declinations remained controlled by the magnetic field; however, this is not indicated by the preliminary anisotropy report [18] since the conclusions were based on declinations only. Correlations of VGP latitude changes as seen from different sampling sites may provide a means to assess the magnitude of a shallowing effect. This hypothesis will be addressed in detail in a separate paper.

In any case, we are left with the observation that both sections in the Confidence Hills recorded similar successive changes in the geomagnetic field during the transition. It would be difficult to argue for a mechanism other than the geomagnetic field which could align magnetic particles in these two sedimentary environments 1.6 km apart. Although one could imagine water currents similarly aligning particles across large distances in some settings, it is highly unlikely that water currents played any role in the alignment of particles in the depositional environments described by Beratan et al. [23] for the Confidence Hills sediments.

## 6. Conclusions

In contrast to the conclusions of a recent anisotropy study [18], traditional tests of the paleomagnetic record in the Confidence Hills show that the upper Olduvai transitional directions are representative of the geomagnetic field. A consistent pat-

tern in the upper Olduvai transitional data is seen across changes in depositional environment, lithology, and structural tilting. VGP's lie within longitudinal bands approximately  $\pm 90^\circ$  away from the sampling site longitude. These bands are substantially different from those found in other studies of the upper Olduvai transition, and do not coincide with the so-called preferred bands of VGP longitude [1-3].

A comparison of all upper Olduvai studies indicate a consistency in the separation of VGP paths from sampling site longitudes. This site dependency lends support to the idea that paleomagnetic inclinations in sediments are greatly shallowed during periods of low field intensity [15]. This does not require that all of these records are incorrect or that they do not record any information about the geomagnetic field during transitions. Our study shows that although VGP's are  $90^\circ$  away from the sampling site and that remanence declinations may follow anisotropy declinations more closely during the transition [18], some part of the geomagnetic field is clearly recorded by the sediments.

In order to resolve the contradictions arising from apparent site-dependency, potential anisotropy issues, and traditional field tests, we need the complete array of paleomagnetic tools and methods. Redeposition experiments using the sediments found in these transition zones may provide useful information about their ability to preserve magnetic directions in the presence of weak fields. In addition, there are other reversals recorded in these Confidence Hills sections (Fig. 6). Comparisons of the paleomagnetic records and magnetic fabric relationships of these other reversals will certainly play a major role in this effort.

## Acknowledgements

We first thank Bob Adams for leading us to the Confidence Hills and pointing out their potential. We are grateful to Kathi Beratan, Jean Hsieh and Bruce Murray for all of their important work on the sedimentary record, and to Chris Pluhar for the initial paleomagnetic survey. Special thanks are due to Liz Warner Holt for field assistance and proofreading, and to Toshitsugu Yamazaki for assisting in mag-



netic separations and for performing TEM work. Helpful comments on the manuscript were received from two anonymous reviewers. We appreciate the National Park Service allowing us to take paleomagnetic samples within the former Death Valley National Monument. We made extensive use of software provided by Craig Jones (cjones@mantle.colorado.edu) for the analysis and presentation of paleomagnetic data, and the GMT package [39] for global projections of VGP's. We appreciate obtaining the reversal atlas [37] from Joanna Athanassopoulos. Work on this project was funded by NSF grant No. EAR-9019289. This is California Institute of Technology Contribution No. 5436. [MK]

## References

- [1] B.M. Clement, Geographical distribution of transitional VGP's: evidence for non-zonal equatorial symmetry during the Matuyama-Brunhes geomagnetic reversal, *Earth Planet. Sci. Lett.* 104, 48-58, 1991.
- [2] C. Laj, A. Mazaud, R. Weeks, M. Fuller and E. Herrero Bervera, Geomagnetic reversal paths, *Nature* 351, 447, 1991.
- [3] E. Tric, C. Laj, C. Jehanno, J.P. Valet, C. Kissel, A. Mazaud and S. Iaccarino, High resolution record of the Upper Olduvai Transition from Po Valley (Italy) sediments: support for dipolar transition geometry?, *Phys. Earth Planet. Inter.* 65, 319-336, 1991.
- [4] K.S. Burakov, B.Z. Gurarii, A.N. Kramov, G.N. Petrova, G.V. Rossanova and V.P. Rodionov, Some peculiarities of the virtual pole positions during reversals, *J. Geomagn. Geoelectr.* 28, 295-307, 1976.
- [5] E. Herrero-Bervera, Some aspects of the geomagnetic field during polarity transitions, Ph.D. Thesis, Univ. Hawaii, 202 pp., 1984.
- [6] B.M. Clement and D.V. Kent, A comparison of two sequential geomagnetic polarity transitions (upper Olduvai and lower Jaramillo) from the Southern Hemisphere, *Phys. Earth Planet. Inter.* 39, 301-313, 1985.
- [7] B.M. Clement and D.V. Kent, Geomagnetic polarity transition records from five hydraulic piston core sites in the North Atlantic, *Init. Rep. DSDP 94*, 831-852, 1986.
- [8] E. Herrero-Bervera and F. Theyer, Non-axisymmetric behaviour of Olduvai and Jaramillo polarity transitions recorded in north-central Pacific deep-sea sediments, *Nature* 322, 159-162, 1986.
- [9] K.A. Hoffman, Long-lived transitional states of the geomagnetic field and the two dynamo families, *Nature* 354, 273-277, 1991.
- [10] T.-Q. Lee, Study of the polarity transition record of the upper Olduvai event from Wulochi sedimentary sequence of the costal range, eastern Taiwan. *TAO* 3, 503-518, 1992.
- [11] C. Constable, Link between geomagnetic reversal paths and secular variation of the field over the past 5 Myr, *Nature* 358, 230-233, 1992.
- [12] C. Laj, A. Mazaud, R. Weeks, M. Fuller and E. Herrero Bervera, Statistical assessment of the preferred longitudinal bands for recent geomagnetic reversal records, *Geophys. Res. Lett.* 19, 2003-2006, 1992.
- [13] J.P. Valet, P. Tucholka, V. Courtillot and L. Meynadier, Paleomagnetic constraints on the geometry of the geomagnetic field during reversals, *Nature* 356, 400-407, 1992.
- [14] P.L. McFadden, C.E. Barton and R.T. Merrill, Do virtual geomagnetic poles follow preferred paths during geomagnetic field reversals?, *Nature* 361, 342-344, 1993.
- [15] X. Quidelleur and J.-P. Valet, Paleomagnetic records of excursions and reversals: possible biases caused by magnetization artefacts, *Phys. Earth Planet. Inter.* 82, 27-48, 1994.
- [16] V. Courtillot and J. Besse, Magnetic field reversals, polar wander, and core-mantle coupling, *Science* 237, 1140-1147, 1987.
- [17] G.D. Egbert, Sampling bias in VGP longitudes, *Geophys. Res. Lett.* 19, 2353-2356, 1992.
- [18] X. Quidelleur, J. Holt and J.-P. Valet, Confounding influence of magnetic fabric on sedimentary records of afield reversal, *Nature* 374, 1995.
- [19] B.C. Burchfiel and J.H. Stewart, "Pull-apart" origin of the central segment of Death Valley, California, *Geol. Soc. Am. Bull.* 77, 439-442, 1966.
- [20] L.A. Wright and B.W. Troxel, Geology of the northern half of the Confidence Hills 15-minute quadrangle, Death Valley region, eastern California: The area of the Amargosa chaos, *Calif. Div. Mines Geol., Map Sheet* 34, 1984.
- [21] B.W. Troxel and P.R. Butler, Multiple Quaternary deformation, central part of the Confidence Hills, Death Valley, California: an example of folding along a strike-slip fault zone., *Quaternary Tectonics of Southern Death Valley, California Field Trip Guide*, 1986.
- [22] L.F. Noble, Structural features of the Virgin Spring area, Death Valley, California, *Bull. Geol. Soc. Am.* 52, 941-999, 1941.
- [23] K. Beratan, J. Hsieh and B. Murray, Pliocene/Pleistocene stratigraphy and depositional environments, southern Confidence Hills, Death Valley, California, *Geol. Soc. Am. Spec. Pap. Cenozoic Basins of the Death Valley Region*
- [24] B.W. Troxel, A.M. Sarna-Wojcicki and C.E. Meyer, Ages, correlations, and sources of three ash beds in deformed Pleistocene beds, Confidence Hills, Death Valley, California., *Quaternary Tectonics of Southern Death Valley, California Field Trip Guide*, 1986.
- [25] A.M. Sarna-Wojcicki and M.S. Pringle, Laser-fusion  $^{40}\text{Ar}/^{39}\text{Ar}$  ages of the Tuff of Taylor Canyon and Bishop Tuff, E. California-W. Nevada, *EOS Trans.*, 1992 Fall Meet. 73, 633, 1992.
- [26] F.J. Hilgen, Astronomical calibration of Gauss to Matuyama sapropels in the Mediterranean and implications for the geomagnetic polarity time scale, *Earth Planet. Sci. Lett.* 104, 226-244, 1991.
- [27] J.L. Kirschvink, The least-squares line and plane and the

- analysis of paleomagnetic data: examples from Siberia and Morocco, *Geophys. J. R. Astron. Soc.* 62, 699-718, 1480.
- [28] S. Cisowski, Interacting vs. non-interacting single-domain behavior in natural and synthetic samples, *Phys. Earth Planet. Inter.* 26, 56-62, 1981.
- [29] S.K. Banerjee, J. King and J. Marvin, A rapid method for magnetic granulometry with applications to environmental studies, *Geophys. Res. Lett.* 8, 333-336, 1981.
- [30] T.C. Onstott, Application of the Bingham distribution function in paleomagnetic studies, *J. Geophys. Res.* 85, 15001510, 1980.
- [31] W. Lowrie and M. Fuller, On the alternating field demagnetization characteristics of multidomain thermoremanent magnetization in magnetite, *J. Geophys. Res.* 76, 6339-6349, 1971.
- [32] S. Levi and R.T. Merrill, Properties of single domain, pseudosingle domain, and multidomain magnetite, *J. Geophys. Res.* 83, 309-323, 1978.
- [33] W.B. Harland, R.L. Armstrong, AN. Cox, L.E. Craig, A.G. Smith and D.G. Smith, *A Geologic Time Scale*, 264 pp., Cambridge Univ. Press, Cambridge, 1989.
- [34] P.L. McFadden and M.W. McElhinny, Classification of the reversal test in paleomagnetism, *Geophys. J. Int.* 103, 725729, 1990.
- [35] N.I. Fisher, T. Lewis and B.J.J. Embleton, *Statistical Analysis of Spherical Data*, 329 pp., Cambridge Univ. Press, Cambridge, 1987.
- [36] A. Cox, The frequency of geomagnetic reversals and the symmetry of the non-dipole field., *Rev. Geophys. Space Phys.* 13, 35-50, 1975.
- [37] J. Athanassopoulos, M. Fuller, R. Weeks and LS. Williams, Atlas of reversal records, EOS, *Trans. Am. Geophys. Union* 74, 109, 1993.
- [38] A. Chauvin, P. Roperch and R.A. Duncan, Records of geomagnetic reversals from volcanic islands of French Polynesia, 2. Paleomagnetic study of a flow sequence (1.2-0.6 Ma) from the island of Tahiti and discussion of reversal models, *J. Geophys. Res.* 95, 2727-2752, 1990.
- [39] P. Wessel and W.H.F. Smith, Free software helps map and display data, EOS, *Trans. Am. Geophys Union* 72, 445-446, 1991.